

Development of femtosecond X-ray source in helium atmosphere with millijoule high-repetition-rate femtosecond laser

Masaki Hada¹ and Jiro Matsuo²

¹Department of Nuclear Engineering, Kyoto University, Sakyo, Kyoto, Japan 606-8501
Fax: 81-774-38-3978, e-mail: hadamasaki@nucleng.kyoto-u.ac.jp

²Quantum Science and Engineering Center, Kyoto University, Gokasho, Uji, Kyoto, Japan 611-0011
Fax: 81-774-38-3978, e-mail: matsuo@nucleng.kyoto-u.ac.jp

High intensity Cu K α X-ray was generated in helium at atmospheric pressure (760 torr) using a commercial millijoule high-repetition rate Ti: sapphire laser. The characteristic K α X-ray was generated by focusing the 0.06 mJ–1.46 mJ, 100 fs and 1 kHz repetition femtosecond laser onto a solid Cu target to a spot with a 5 μ m diameter. We obtained the characteristic K α X-ray of 5.4×10^9 photos/s into 2π sr at a 1 kHz repetition rate with 5.0×10^{-6} conversion efficiency. K α X-ray intensity can be enhanced with 4–8% prepulse plasma into 7.7×10^9 photos/s/sr with 6.8×10^{-6} conversion efficiency. The X-ray intensity and conversion efficiency in helium achieved the almost the same level as in vacuum. Such vacuum-free femtosecond X-ray source with a tabletop laser can be a promising and easy accessible tool for time-resolved X-ray diffraction and other radiographic applications. The time-resolved X-ray diffraction experiment would reveal the ultrafast dynamics in crystalline materials, such as coherent phonon vibrations and ultrafast phase transitions.

Key words: laser-induced plasma, X-ray, ultrafast science, femtosecond laser

1. INTRODUCTION

Hard X-ray from femtosecond laser-produced plasma has gained much interest, as unique time resolved X-ray diffraction (XRD) experiments demonstrate and reveal the atomic dynamics of chemical reactions, phase transitions and coherent phonon vibrations.[1-4] Those X-ray diffraction and other X-ray radiographic applications such as the time-resolved X-ray absorption fine structure experiment would reveal the ultrafast dynamics of coherent phonon vibrations and ultrafast phase transitions, but also the structural dynamics of light-sensitive organic materials. A variety of femtosecond X-ray sources has been developed, such as laser-produced plasma X-ray source, ultrafast hard X-ray produced by synchrotron and XFEL.[3,5-6] The intensity or coherency of X-ray in synchrotrons or XFEL is quite high, however, the instruments are very expensive and it is required huge and complex facilities; moreover, the availability of those huge facilities is limited. Laser-produced plasma X-ray source are required to be comparatively small, lab-scale facility. Laser-produced plasma X-ray sources have consisted of high-power (above 100 millijoule) and low-repetition-rate (about 10 Hz) lasers and the K α -X-ray intensity using this large size laser was reported to be 10^8 – 10^{11} cps/sr with conversion efficiency of 10^{-4} – 10^{-5} . [7-10] Generally an X-ray intensity of more than several 10^8 cps/sr is required for time-resolved XRD experiments, and a laser-plasma X-ray of 10^9 – 10^{11} cps/sr is desirable.[11] This intensity is sufficiently high for the X-ray radiographic applications. Nevertheless, the utilization of such

ultrafast pulsed X-ray has been limited because of the complexity of the huge vacuum system and difficulty in managing a high-power laser. To date, a huge laboratory-top laser and a large size vacuum chamber are requisites to generate ultrafast pulsed X-ray radiation. In this laboratory-scale ultrafast X-ray source, there are also some problems with target forms and debris from the target caused by laser ablation. Regarding the target form, thin tape or wire typed targets have been used because the space in the vacuum chamber is limited. The small tape or wire target can be put in a vacuum chamber; however target lifetime is quite short at about several hours or at most a few days. It is difficult to control the surface of the thin tape or wire within a few micrometers. There is also the problem of debris from the target. When the high-power laser is focused onto the target, target materials are blown off and deposited on the focusing lens, windows, and other optics. Thin polymer tape covers have been employed to avoid the debris problem. Thus, such ultrafast pulsed X-ray sources were required to be more compact, easier to access, and have higher conversion efficiency into characteristic X-ray.

Recently, the compact designed tabletop submillijoule to several millijoule femtosecond laser has been reported to be available for generating hard X-ray with an intensity of about 10^8 – 10^{10} cps/sr with the K α X-ray conversion efficiency of 10^{-5} – 10^{-6} . [12-14] Although the experimental scale of a femtosecond laser could be successfully reduced with a tabletop femtosecond laser, difficulties remain when using

	synchrotron X-ray	laser-induced plasma X-ray		
		High Power (>100mJ)	Low Power (~1mJ)	
size of the facility	facility-top	laboratory-top	table-top	
Laser forcing condition		in vacuum condition		in atmospheric condition
X-ray intensity	$10^{15} \sim 10^{17}$ cps/mm ² ·(mrad) ² ·0.1%	$10^8 \sim 10^{11}$ cps/sr	$10^8 \sim 10^{10}$ cps/sr	$10^8 \sim 10^9$ cps/sr
X-ray conversion efficiency (K _α X-ray)		$10^{-4} \sim 10^{-5}$ [7-10]	$10^{-5} \sim 10^{-6}$ [12-14]	$\sim 10^{-6}$ [16,17,this work]
available pulse duration (estimation)	100 fs – 100 ps [3]	200 fs – 2 ps [18]	100 fs – 2 ps [18]	100 fs – 2 ps [18]
cost	extremely high	high	low	low
user-convenience	huge facility limitation of utilities	huge laser system complexity in utility of vacuum	compact laser system complexity in utility of vacuum	compact laser system no vacuum system

Table 1: General comparison of the laser-induced plasma X-ray with low-power femtosecond laser with X-ray from synchrotron and high-power femtosecond laser.

a huge and complex vacuum chamber system; such as target manipulation, target lifetime, and debris emissions. Therefore, a high-intensity X-ray source that can operate in atmospheric pressure (760 torr) with a tabletop laser could be a desirable tool for ultrafast time-resolved measurements. Laser-induced plasma X-ray sources in helium atmospheric condition have been reported, however the X-ray intensity from these sources was quite low.[15] Very recently, J. A. Nees *et al.* has been developed a high intensity X-ray source ($\sim 5 \times 10^9$ cps) in helium atmospheric condition at the high plasma intensity of above 1.0×10^{18} W/cm². [16,17] Nevertheless, the high intensity plasma above 1.0×10^{18} W/cm² would extend the pulse duration of X-ray up to picosecond order.

The plasma intensity generated on the laser focusing spot, is the key parameter for the pulse duration of the laser-induced plasma X-ray. The plasma intensity is calculated with the laser power of a single pulse, its pulse duration and the diameter of focusing spot. As for the pulse duration of pulsed X-ray, computer simulated study has been demonstrated that the pulse duration of X-ray was extended with increase of the laser plasma intensity.[18] At the plasma intensity of 1.0×10^{16} W/cm² and 1.0×10^{18} W/cm², the extension of pulse duration was ~ 100 fs and ~ 1 ps respectively. Therefore, laser-induced plasma source with lower (at most 5.0×10^{16} W/cm²) plasma intensity is required for the time-resolved X-ray diffraction applications. Experimental methods for the pulse duration measurement are the ultrafast streak camera measurement and the pump-probe measurement of ultrafast dynamics. The pulse duration of ultrafast X-ray is directly measured with the streak camera. In the streak camera lights are changed into electrons and the electrons are accelerated and detected with the detector. In this process, the generated electrons have wide-range energy and it makes the pulse duration resolution of streak camera more than a few picoseconds. Thus until now, in order to measure the pulse duration of ultrafast X-ray precisely, it is required to observe the ultrafast change of X-ray diffraction patterns. In Table 1, we summarized the general comparison among the X-ray

from synchrotron and laser-induced plasma X-ray with high power and low power femtosecond laser.

When a high-intensity laser pulse is focused onto a target, at first the pulse changes the surface of the target into near-solid-density plasma by ionization of surface constituents. The absorption process of the laser pulse into the surface materials varies with the intensity of the laser pulse. For plasma intensities in the range $1\lambda^2 < 4 \times 10^{16}$ W $\mu\text{m}^2/\text{cm}^2$, laser-produced plasmas are reported to be absorbed into the target via collisionless processes such as resonant absorption.[19-23] Hot electrons in the produced laser plasma are interacted with the incident laser pulse and are accelerated into the solid target. As the high energy electrons are penetrate into the target material, X-rays are generated via ionization of target material by the high energy electrons or bremsstrahlung. This X-rays are generated when hot electron are on the surface of the target; thus, the pulse duration of the laser-produced X-ray is similar to the incident laser pulse, i.e., several hundred fs. This laser-produced plasma has the potential of a unique, wide range of energy electron and sub-keV to 100 keV range of hard X-ray source.

The generated X-ray intensity is enhanced with prepulse, which produces very weak plasma on the target surface prior to the main pulse.[12,24-27] The mechanism of X-ray intensity enhancement with prepulse is explained by the strong interaction between electrons in the preplasma and the main laser pulse. The prepulse produces weak plasma on the surface of the target and electrons in the plasma are gradually expand from the surface within a distance of more than a few micrometers in the time scale of 10–100 ps. Then, the main pulse enters the plasma and the dispersed electrons are accelerated into the target surface. It has been reported that the X-ray intensity with prepulse enhancement is three to ten times higher than with only a main pulse, and the time separation between prepulse and main pulse is on the order of 10–100 ps.[12,27]

Regarding prepulse, there is an advantage and disadvantage; the advantage is improving the X-ray yield and the disadvantage is the extension of the X-ray pulse duration. The electrons in plasma can expand from the surface to distance of more than 30 μm even in low vacuum pressure of 10 torr. A traveling distance of more than 30 μm from the surface at the speed of light indicates that the pulse duration extension was more than 100fs.

In this study, we demonstrated a compact and high-intensity ultrafast pulsed X-ray source constructed in a helium atmosphere at plasma intensity (effective) of $1.0\text{--}4.0 \times 10^{16} \text{ W}\mu\text{m}^2/\text{cm}^2$. It is possible to reduce the overall size of the X-ray source system without the complexity of a vacuum system. It is also feasible to set a long-lived and large-sized target regardless of the vacuum chamber in air. The samples measured with time-resolved XRD are placed close to the X-ray generating spot without a vacuum system, enabling the efficiently use of the generated X-ray. This vacuum-free X-ray system allows us to avoid the debris problem. At atmospheric pressure, the debris cannot reach the focusing lens or other optics, which are placed some ten millimeters away from the focusing spot. With helium or other gas jet, the debris can be easily collected with a filter.

2. EXPERIMENTAL

Fig. 1 shows the experimental setup for ultrafast pulsed X-ray generation with various prepulse time separations. The mode-locked Ti:sapphire laser generated femtosecond optical pulses of about 100 fs duration with wavelength at 800 nm, and the optical pulses were amplified at about 3.5 mJ/pulse through a regenerative amplifier (Spectra Physics / Model Spitfire Pro XP) with repetition rate of 1 kHz. The laser pulse profile was TEM₀₀ and it was *p*-polarized. The optical pulse had a prepulse which was generated in the regenerative amplifier laser system itself, as leakage through the Pockels cell before the final pulse of the pulse train was switched off. The prepulse contrast to the main pulse was measured to be 8×10^{-4} , and the time separation between the prepulse and main pulse was 20 ns. The influence of the prepulse plasma on X-ray generation is negligible in this time regime of ten nanoseconds prepulse even if the prepulse generates preplasma on the target surface.[12]

The optical pulse generated through the regenerative amplifier was separated by the 1:9 beam splitter. The stronger pulse was changed its polarization by the first $\lambda/2$ waveplate and was reflected in the part of the *s*-polarized pulse by the polarized mirror. The intensity of the main pulse can be varied with this polarized mirror. The main pulse changed its polarization to *p* by the second $\lambda/2$ waveplate and penetrated a polarized beam splitter that reflected the *s*-polarized beam 30% and let the *p*-polarized beam go through. The weaker pulse for inducing

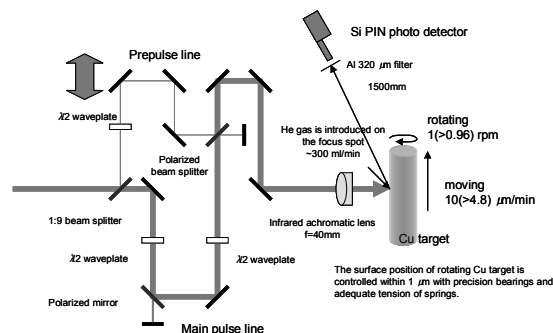


Fig.1: The experimental setup for ultrafast pulsed X-ray generation with various prepulse time separations.

preplasma changed its polarization into *s*, went through an optical delay line, and was reflected by the polarized beam splitter. The main pulse and prepulse were brought in the same line and focused into a rotating copper target with an infrared achromatic lens ($f = 40 \text{ mm}$, N.A. = 0.2). The focusing spot size was 5 μm , which was measured by the crater size of the focusing spot. This spot size was well corresponded to the diffraction limit of this infrared achromatic lens (4.8 μm). The pulse duration of the laser pulse on the surface of copper target was 100 fs. The power of the optical main pulse was 0.06 mJ – 1.46 mJ and the power of prepulse was fixed 0.06 mJ. The copper target was a circular cylinder of 100 mm diameter and 300 mm length. The surface position of rotating copper target was controlled within $\pm 1 \mu\text{m}$ with precision bearings and adequate tension of springs, and was measured with a micrometer during rotation. The copper target rotates at a rate of 1 (> 0.96) rpm, which could be varied in the range 0.24–1 rpm and moves in the axial direction at the rate of 10 (> 5) $\mu\text{m}/\text{min}$, which gives a fresh copper surface with each laser shot. An X-ray generating operation of more than 20 days can be available with this long-life copper target. Near the focus point atmosphere in the Cu target system can be changed between air and helium. The helium gas was introducing with 1/4 inches gas nozzle and the flow rate of helium gas was 500 ml/min. In air, the debris from the target was not deposited on the focusing lens or other optics. We also made same X-ray generation system with Cu target in a vacuum chamber to compare with the X-ray intensity at atmospheric pressure in air and under vacuum (20 mtorr).

The X-ray generated from focusing the laser pulse onto a copper target was measured with a PIN-Si photo detector (Amptek / XR-100CR) which has a 300 μm thick, 7 mm² square silicon sensor. The detection efficiency of this PIN-Si photo detector is approximately 100% for an 8 keV X-ray. The detector was sealed with 25 μm thickness Be window through which 8 keV X-ray passes without any losses. A spectroscopy amplifier (CANBERRA / 2022 Spectroscopy Amplifier) was used to amplify the signal, which

was tallied up with a multichannel analyzer (SEIKO EG&G / TRUMP-MCA-2k). The detector was placed 1500 mm away from the focusing spot at an angle of 60° . In a vacuum condition, the X-ray went through 3 mm in vacuum and 1497mm in air. In helium atmosphere or in vacuum conditions, a thin aluminum filter of $320 \mu\text{m}$ was placed before the detector. This filter reduces the X-ray intensity to 1.72% for a Cu $K\alpha$ X-ray. The long distance between the X-ray focusing spot and the detector and the Al filter allowed us to measure the X-ray photons as a Poisson distribution single photon counting. Two different photons cannot be detected at once in the order of 1 millisecond using a Si photo detector and multichannel analyzer. If more than one photon is in the same detecting time, the total energy of the photons will be measured with the Si photo detector. In any conditions, it took 40 s to obtain each X-ray spectrum.

3. RESULTS AND DISCUSSION

The typical X-ray spectrum obtained with the Si-PIN photo detector is shown in Figure 2. The dashed line with square symbols is the X-ray spectrum measured with the Si-PIN photo detector. The X-ray generated on the focusing spot went through 1500 mm air and $320 \mu\text{m}$ Al filter (in He atmosphere or in vacuum condition), thus the X-ray intensity were reduced depending on their energy to obtain the single photon counting. The solid line with circle symbols was calculated X-ray spectrum. X-ray radiation from p -polarized laser is regarded as isotropic radiation.[28] As shown by the solid line of Figure 2, the strong Cu $K\alpha$ X-ray line (8.05 keV), $K\beta$ X-ray line (8.91 keV) and a small part of the bremsstrahlung X-ray were found in the energy range of several keV.

In Figure 3, the $K\alpha$ intensity was plotted as a function of the plasma intensity in various atmospheric conditions. The plasma intensity was varied from 1.5×10^{15} – $4.0 \times 10^{16} \text{ W}\mu\text{m}^2/\text{cm}^2$ to change the incident laser pulse energy in the range 0.06–1.46 mJ/pulse by rotating the first $\lambda/2$ waveplate of the main pulse line in Figure 1. At this plasma energy, the laser absorption process into the target is collisionless. The polarized mirror in the main pulse line lets p -polarized light pass through and s -polarized light be reflected. In this condition, the prepulse line was blocked and the influence of the preplasma was negligible. We obtained high intensity Cu $K\alpha$ X-rays with 2.6 – 5.4×10^9 photons/sr/s above the plasma intensity of $2.0 \times 10^{16} \text{ W}\mu\text{m}^2/\text{cm}^2$ in He atmosphere. This intensity was more than 60 times that in air, and close to the intensity of 1.2 – 1.8×10^{10} photons/sr/s obtained in vacuum. Generally, a value of at least several 10^8 cps/sr characteristic X-ray is required for time-resolved XRD or other applications. In Figure 3, the horizontal dashed line shows the X-ray intensity of 1.0×10^9 cps/sr. We obtained an intensity of 5.4×10^9 cps/sr in helium atmosphere, which is

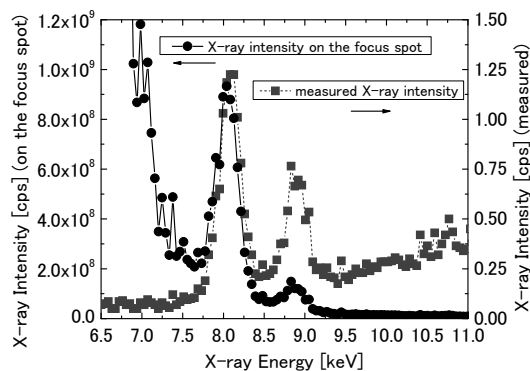


Fig.2: Typical X-ray spectrum. The dashed line with square symbols is measured X-ray spectrum with Si-PIN photo detector, and the solid line with circle symbols is the X-ray spectrum calculated from the X-ray intensity reduction by the air layer and Al filter.

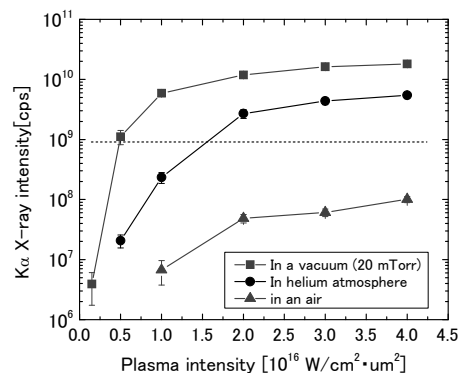


Fig.3: $K\alpha$ X-ray intensity in various atmospheres; solid line with square: vacuum (20 mtorr), solid line with circles: in helium, solid line with triangle: in air

sufficiently high for time-resolved X-ray measurements.

The relationship between X-ray intensity and the condition of the atmosphere can be approximately explained with the mean free path of electrons according to the collision model of diatomic molecules.[29] The electrons in the plasma produced by the incident laser pulse expand several micrometers. If the electrons collide with the atoms/molecules of the atmosphere gas and lose their energy before or during acceleration with the incident pulse, the electrons can not reach the surface of the target and also cannot produce X-rays. In this collision model of diatomic molecules, the number of electrons decreases exponentially as the electrons move in the atmosphere. Thus, the X-ray intensity can be expressed by the equation $I = I_0 \exp(-A/\lambda)$. Here, I_0 is the intensity of the X-ray generated on the target, I is the intensity of the measured X-ray in the atmosphere, and A and λ are the traveling

length and electron mean free path in the atmosphere, respectively. In this focusing condition, electrons travel with the velocity of the light about 1.47 μm in atmosphere gases; A is 1.47 μm . [29] The electron mean free path in vacuum conditions (20 mtorr) is 13 mm and I/I_0 is 100% without any loss of diatomic molecules in this collision model, while the electron mean free path in helium is 1.01 μm and 0.34 μm in air. Therefore, the intensity ratio I/I_0 is about 30% in helium and 1% in air. The X-ray intensity that can be obtained in air is only 1% of that in vacuum, i.e., $1.2\text{--}1.8 \times 10^{10}$ cps/sr. This means that $K\alpha$ X-ray intensity of at most 1.8×10^8 cps/sr can be obtained in air which is smaller than several 10^8 cps/sr and quite difficult to use for the time-resolved X-ray measurements. The $K\alpha$ X-ray intensity observed in a helium atmosphere was $2.6\text{--}5.4 \times 10^9$ cps/sr, which is about 30% of $1.2\text{--}1.8 \times 10^{10}$ cps/sr measured in a vacuum. This intensity is sufficiently high for the required intensity of several 10^8 cps/sr. Thus, it is possible to utilize the $K\alpha$ X-ray generated at atmospheric pressure in helium for the time-resolved XRD or other applications.

X-ray intensity can be enhanced with prepulse plasma because of the strong coupling between the laser pulse and preplasma generated with prepulse. The intensity of preplasma was 1.6×10^{15} $\text{W}\mu\text{m}^2/\text{cm}^2$ which was 4-8% of the main plasma power between 2.0×10^{16} $\text{W}\mu\text{m}^2/\text{cm}^2$ and 4.0×10^{16} $\text{W}\mu\text{m}^2/\text{cm}^2$, and the separation time between the prepulse and the main pulse was 5 ps. Above the plasma intensity of 2.0×10^{16} $\text{W}\mu\text{m}^2/\text{cm}^2$, the obtained X-ray intensities with prepulse were 1.3 times higher in helium and 2.0 times higher in air. The $K\alpha$ X-ray intensity obtained in helium with prepulse was 7.7×10^9 cps/sr, which was 40% of the yield in a vacuum without prepulse. In a vacuum, the $K\alpha$ X-ray intensity with prepulse enhancement has been reported to be three to ten times higher than with the main pulse only. [12,27] The prepulse enhancement effect of $K\alpha$ X-ray intensity in a helium atmosphere was smaller than that in a vacuum. At plasma intensity of 3.0×10^{16} $\text{W}\mu\text{m}^2/\text{cm}^2$ in helium at atmospheric pressure, the X-ray intensity with prepulse in helium was almost constant for any separation time during 1-50 ps. However, the prepulse enhancement in vacuum was reported to be higher and to have a peak in the function of the pulse separation time in the range of 30-50 ps. [12,27]

This result can be also explained with collision of diatomic molecules. In vacuum conditions, electrons generated by preplasma can expand from a few to several micrometers from the target surface because of the electron mean free path of below 1 mm to 100 mm. Then, the electrons in preplasma can be accelerated by the main pulse and produce X-rays. However, in helium at atmosphere pressure, the electrons in preplasma can travel only 1-2 μm from the surface because the electron mean free path is 1.01 μm . Almost

all electrons in the preplasma interact with helium atoms and lose their energy. A small amount of electrons with very slow velocity remain in the near-surface region of the target and can be accelerated with the main pulse. These electrons produce the X-ray with a prepulse enhancement value of 1.3. Even though a prepulse enhancement of 1.3 times was observed in helium at atmospheric pressure, it is better to construct the X-ray generation systems without prepulse line. As shown in Figure 1, there are some optical loss for building the prepulse line: 10% loss by the 1:9 beam splitter, 10% loss by the polarized beam splitter, and a few percents loss by the additional mirrors required to let the main pulse and prepulse pass through the same line. The total loss from constructing such a complex main pulse and prepulse line amounts to more than 30%. Thus, by removing the prepulse line and increasing the main laser power, an X-ray intensity 1.3 times higher than without prepulse with plasma power of 4.0×10^{16} $\text{W}\mu\text{m}^2/\text{cm}^2$ can be obtained in helium at atmospheric pressure.

Above the plasma intensity of 2.0×10^{16} $\text{W}\mu\text{m}^2/\text{cm}^2$, the $K\alpha$ X-ray conversion efficiency calculated from the X-ray intensity and incident pulse energy in helium at atmospheric pressure was $5.0 (\pm 0.2) \times 10^{-6}$, a value 60 times higher than that in air (8.2×10^{-8}) and close to the value in a vacuum ($1.8\text{--}2.1 \times 10^{-5}$). A $K\alpha$ conversion efficiency of 10^{-6} to 10^{-5} is also need to obtain X-ray intensity of more than several 10^8 cps required for time-resolved XRD. However, in air the $K\alpha$ X-ray intensity or conversion efficiency was quite low; in helium at atmospheric pressure, the $K\alpha$ X-ray intensity and conversion efficiency achieved the value of 5.4×10^9 cps and 5.0×10^{-6} , which are sufficiently high for time-resolved XRD or other X-ray applications. This vacuum-free, compact and easy-to-access X-ray generation system can be operated in helium at atmospheric pressure. The conversion efficiency obtained by other groups using high repetition millijoule or submillijoule laser has been reported to be about $4.6 \times 10^{-6}\text{--}3.2 \times 10^{-5}$. [12-14] in vacuum conditions and $\sim 5.0 \times 10^{-6}$ in helium atmospheric conditions. The $K\alpha$ X-ray intensity obtained in helium at atmospheric pressure was also of the same order as the other works using high repetition millijoule or submillijoule laser in vacuum conditions. Thus this compactly designed high-intensity $K\alpha$ X-ray source that can operate at atmospheric pressure without using a large and complex vacuum chamber can be a useful and promising tool for the time-resolved XRD or other radiographic applications.

4. CONCLUSION

High intensity $K\alpha$ X-ray generation at a high repetition was demonstrated with tabletop commercial ultrafast laser system in helium at atmospheric pressure. Millijoule, 100 fs laser pulses were focused onto a well-controlled Cu

surface at intensities of 5×10^{15} to 4×10^{16} $W\mu m^2/cm^2$. The intensity of the generated $K\alpha$ X-ray in helium at atmospheric pressure was 5.4×10^9 cps/sr with 1 kHz repetition rate and conversion efficiency of 5.0×10^{-6} . This X-ray intensity is close to that obtained in vacuum condition and is high enough for the time-resolved XRD or other X-ray applications. The $K\alpha$ X-ray intensity was enhanced with 4–8% prepulse plasma into 7.7×10^9 cps/sr and 6.8×10^{-6} conversion efficiency. Regarding the prepulse, it would be better to construct a simpler X-ray generation system without the prepulse line because of the optical losses in the system. Such a high-intensity, vacuum-free femtosecond X-ray source with a tabletop laser could be a promising tool for the time-resolved XRD or other radiographic applications.

ACKNOWLEDGEMENTS

This work is partially supported by the JST, CREST. We would like to thank Dr. T. Aoki, Dr. T. Seki, Dr. S. Ninomiya, Mr. K. Ichiki, Mr. H. Yamada, Mr. Y. Yamamoto, Mr. T. Yamanobe, Mr. Y. Wakamatsu and Ms S. Ibuki from Kyoto University for discussing X-ray generation systems.

REFERENCES

- [1] C. Rose-Petruck, R. Jimenez, T. Guo, A. Cavalleri, C. W. Siders, F. Raksi, J. A. Squier, B. C. Walker, K. R. Wilson, C. P. J. Barty, *Nature (London)* **398**, 310-312 (1999).
- [2] K. Sokolowski-Tinten, C. Blome, J. Blums, A. Cavalleri, C. Dietrich, A. Tarasevitch, I. Uschmann, E. Forster, M. Kammler, M. Horn-von-Hoegen, D. von der Linde, *Nature (London)* **422**, 287-289 (2003).
- [3] A. M. Lindenberg, J. Larsson, K. Sokolowski-Tinten, K. J. Gaffney, C. Blome, O. Synnergren, J. Sheppard, C. Coleman, A. G. MacPhee, D. Weinstein, D. P. Lowney, T. K. Allison, T. Matthews, R. W. Falcone, A. L. Cavalieri, D. M. Fritz, S. H. Lee, P. H. Bucksbaum, D. A. Reis, J. Rudati, P. H. Fuoss, C. C. Kao, D. P. Siddons, R. Pahl, J. Als-Nielsen, S. Duesterer, R. Ischebeck, H. Schlarb, H. Schulte-Schrepping, Th. Tschentscher, J. Schneider, D. von der Linde, O. Hignette, F. Sette, H. N. Chapman, R. W. Lee, T. N. Hansen, S. Techert, J. S. Wark, M. Bergh, G. Hultdt, D. van der Spoel, N. Timneanu, J. Hajdu, R. A. Akre, E. Bong, P. Krejcik, J. Arthur, S. Brennan, K. Luening, J. B. Hastings, *Science* **308**, 392-395 (2005).
- [4] D. M. Fritz, D. A. Reis, B. Adams, R. A. Akre, J. Arthur, C. Blome, P. H. Bucksbaum, A. L. Cavalieri, S. Engemann, S. Fahy, R. W. Falcone, P. H. Fuoss, K. J. Gaffney, M. J. George, J. Hajdu, M. P. Hertlein, P. B. Hillyard, M. Horn-von-Hoegen, M. Kammler, J. Kaspar, R. Kienberger, P. Krejcik, S. H. Lee, A. M. Lindenberg, B. McFarland, D. Meyer, T. Montagne, É. D. Murray, A. J. Nelson, M. Nicoul, R. Pahl, J. Rudati, H. Schlarb, D. P. Siddons, K. Sokolowski-Tinten, Th. Tschentscher, D. von der Linde, J. B. Hastings, *Science* **315**, 633-636 (2007).
- [5] P. Lucas, S. Webber, Eds. (IEEE, Piscataway, NJ, 2003), p. 423-425.
- [6] R. Service, *Science* **298**, 1356-1368 (2002).
- [7] M. Yoshida, Y. Fujimoto, Y. Hironaka, K.G. Nakamura, K. Kondo, M. Ohtani, H. Tsunemi: *Appl. Phys. Lett.* **73**, 2393-2395 (1998).
- [8] E.C. Eder, G. Pretzler, E. Fill, K. Eidmann, A. Saemann: *Appl. Phys. B70*, 211-217 (2000).
- [9] E. Fill, J. Bayerl, R. Tommasini: *Rev. Sci. Instrum.* **73**, 2190-2192 (2002).
- [10] C.W. Siders, A. Cavalleri, K. Sokolowski-Tinten, T. Guo, C. Töth, R. Jimenez, C. Rose-Petruck, M. Kammler, M. Horn von Hoegen, D. von der Linde, K.R. Wilson, C.P.J. Barty: *SPIE Proc.* **3776**, 302-311 (1999).
- [11] K. Sokolowski-Tinten, D. von der Linde, *J. Phys.: Condens. Matter* **16** R1517-1536 (2004)
- [12] C.L. Rettig, W.M. Roquemore, J.R. Gord, *Appl. Phys. B93* 365-372 (2008).
- [13] M. Hagedorn, J. Kutzner, G. Tsilimis, H. Zacharias, *Appl. Phys. B77* 49-57 (2003).
- [14] C. G. Serbanescu, J. A. Chakera, and R. Fedosejevs, *Rev. Sci. Instruments* **78**, 103502 (2007).
- [15] Y. Jiang, T. Lee, W. Li, G. Ketwaroo, and C. G. Rose-Petruck, *J. Opt. Soc. Am. B* **20**, 229-237 (2003).
- [16] B. Hou, J. Easter, K. Krushelnick, and J. A. Nees, *Appl. Phys. Lett.* **92**, 161501 (2008).
- [17] B. Hou, J. Easter, A. Mordovanakis, K. Krushelnick, and J. A. Nees, *Opt. Express* **16**, 17695 (2008).
- [18] Ch. Reich, P. Gibbon, I. Uschmann, and E. Förster, *Phys. Rev. Lett.* **84**, 4846-4849 (2000).
- [19] K. Eidmann, J. Meyer-ter-Vehn, T. Schlegel, and S. Hüller, *Phys. Rev. E* **62**, 1202-1214 (2000).
- [20] R. Fedosejevs, R. Ottmann, R. Sigel, G. Kühnle, S. Szatmari, and F. P. Schäfer, *Phys. Rev. Lett.* **64**, 1250-1253 (1990).
- [21] D. F. Price, R. M. More, R. S. Walling, G. Guethlein, R. L. Shepherd, R.E. Stewart, and W. E. White, *Phys. Rev. Lett.* **75**, 252-255 (1995).
- [22] D. W. Forslund, J. M. Kindel, and K. Lee, *Phys. Rev. Lett.* **39**, 284-288 (1977).
- [23] P. Gibbon and E. Förster, *Plasma Phys. Controlled Fusion* **38**, 769-793 (1996).
- [24] D. Kuhike, U. Herpers, D. von der Linde, *Appl. Phys. Lett.* **50**, 1785-1787 (1987).
- [25] O. R. Wood, W. T. Silfvast, H. W. K. Tom, W. H. Knox, R. L. Fork, C. H. Brito-Cruz, M. C. Downer, P. J. Maloney, *Appl Phys. Lett.* **53**, 654-656 (1988).
- [26] H. Nakano, T. Nishikawa, H. Ahn, and N. Uesugi, *Appl. Phys. Lett.* **69**, 2992-2994 (1996).
- [27] J. Kutzner, M. Sillies, T. Witting, G. Tsilimis, H. Zacharias, *Appl. Phys. B78*, 949-955 (2004).
- [28] Y. Hironaka, K.G. Nakamura, K. Kondo, *Appl. Phys. Lett.* **77** 4110-4111 (2000).
- [29] M. Hada, J. Matsuo, submitting to *Appl. Phys. B*

(Received July 14, 2009; Accepted August 22, 2009)